Carbon 145 (2019) 401–410

Contents lists available at ScienceDirect

Carbon

journal homepage: www.elsevier.com/locate/carbon

# Effect of nickel coating on the stress-dependent electric permittivity, piezoelectricity and piezoresistivity of carbon fiber, with relevance to stress self-sensing

Xiang Xi, D.D.L. Chung*

*Composite Materials Research Laboratory, Department of Mechanical and Aerospace Engineering, University at Buffalo, The State University of New York, Buffalo, NY, 14260-4400, USA*

ARTICLE INFO

*Article history:*
Received 25 October 2018
Received in revised form
28 December 2018
Accepted 8 January 2019
Available online 9 January 2019

ABSTRACT

This paper unprecedentedly reports the effect of metal (nickel) coating on the stress-dependent electric permittivity, piezoelectricity and piezoresistivity of carbon fiber. Both permittivity (2 kHz) and DC conductivity of carbon fiber are increased by nickel coating. For 7-μm diameter carbon fiber, nickel coating (0.25-μm thickness) increases the relative permittivity from 12,200 to 63,200, and decreases the resistivity from $1.5 \times 10^{-5}$ to $1.5 \times 10^{-7}$ Ω.m. The relative permittivity of the nickel coating (Rule of Mixtures) is 404,600 - similar to 405,300 for nickel wire (160-μm diameter). The resistivity of the nickel coating (Rule of Mixtures) is $2.0 \times 10^{-8}$ Ω.m - lower than $8.8 \times 10^{-8}$ Ω.m for the nickel wire - probably because of the higher degree of preferred crystallographic orientation in the nickel coating. The nickel structure affects the conduction more than polarization. The piezoelectric and piezoresistive effects are diminished by the nickel coating, which governs these effects. The nickel coating changes the stress dependence of the permittivity (for capacitance-based self-sensing) from positive to negative and changes the piezoresistivity (for resistance-based self-sensing) from negative (gage factor −1830) to positive (gage factor +1650). The piezoelectricity of the nickel-coated carbon fiber and nickel wire are similar, but the piezoresistivity is weak for the latter (gage factor +30).



## 1. Introduction

Carbon fibers are well-known for their electrical and thermal conductivity, in addition to their low density, high strength and high elastic modulus. Thus, they are used in structural, electrical and thermal applications.

The coating of carbon fibers (or nanofibers) with a metal, most commonly nickel, has long been used to increase the electrical conductivity of the fiber, thereby enhancing numerous properties, particularly (i) the effectiveness of the fiber as an electrically conductive filler in a polymer-matrix composite (for increasing the conductivity of the composite) [1–3] or a cement-matrix composite (for facilitating the cathodic protection of the steel embedded in the composite) [4], (ii) the electromagnetic interference (EMI) shielding effectiveness [5–13], (iii) the lightning protection ability (as needed for aircraft), (iv) the fuel cell electrode effectiveness (lower charge transfer resistance and higher current density) [14,15], and (v) the rapidity of the heating provided by passing an electric current through the fiber (as needed for the deicing and anti-icing of aircraft) [16,17]. Furthermore, the nickel coating provides ferromagnetic behavior [18,19], and facilitates magnetic applications such as magnetic-field-induced alignment of carbon fibers [20]. In addition, nickel-coated carbon fiber fabric serves as an interface material to strengthen the joint between a metal (such as aluminum and titanium) and a carbon fiber polymer-matrix composite [21–23]. However, both enhancement and degradation of the mechanical properties of the fiber composite due to the nickel coating on the fiber have been reported [24,25]. The nickel coating is most commonly deposited on the carbon fiber by electroplating [26,27], though electroless plating [18,28,29], cementation [29] and chemical vapor deposition are alternate processes. Nickel is the most commonly used metal for coating carbon fibers, because of its oxidation resistance. Copper is more conductive than nickel, but its oxidation resistance is inferior. Both nickel and copper are suitable for deposition by electroplating.

* Corresponding author.
*E-mail address:* ddlchung@buffalo.edu (D.D.L. Chung).
*URL:* http://alum.mit.edu/www/ddlchung

https://doi.org/10.1016/j.carbon.2019.01.034
0008-6223/

The electric permittivity (also known as the dielectric constant) is a fundamental material property that affects the alternating current (AC) electrical behavior due to the associated capacitance. It pertains to the electric polarization, which results in a reverse electric field that opposes the applied electric field [30]. The reverse field impedes conduction, whether AC or DC. For any of the electrical applications mentioned above, the permittivity matters. Although the permittivity of some monolithic metals (steels, aluminum and copper) [31–33] and some continuous carbon fibers (PAN-based and mesophase-pitch-based carbon fibers) [34,35] has been reported, the permittivity of metal-coated carbon fiber has not been previously reported for any type of metal. In order to support the numerous electrical and electrochemical applications of metal-coated carbon fibers, this paper is partly directed at determining the permittivity of metal-coated carbon fiber for the first time.

The piezoelectric behavior in the form of the direct piezoelectric effect converts mechanical energy to electrical energy and is useful for stress/strain sensing and mechanical energy harvesting. In addition, the electric field and capacitance resulting from the direct piezoelectric effect can influence the conduction performance, which is central to numerous applications of metal-coated carbon fibers. The piezoelectric behavior of continuous carbon fiber (PAN-based) has been reported recently [35]. Although the piezoelectric coupling coefficient is low ($+1.4 \times 10^{-8}$ pC/N), the effect allows stress sensing through measurement of either the electric field output or the capacitance output [36]. This means self-sensing, i.e., sensing a structure using the structure to sense itself, without the use of embedded or attached sensors. Advantages of self-sensing compared to the use of embedded or attached sensors include low cost, high durability, large sensing volume and absence of mechanical property loss. This paper is partly directed at investigating the piezoelectric behavior of metal-coated carbon fiber for the first time.

The dependence of the permittivity on stress provides a form of piezoelectric behavior, in addition to enabling capacitance-based stress/strain self-sensing. Furthermore, due to the above-mentioned negative effect of the permittivity on electrical conduction, information on the effect of stress on the permittivity is relevant to conduction applications. The increase of the relative permittivity with increasing tensile stress has been previously reported for uncoated carbon fiber [36]. The increase of the relative permittivity with increasing compressive stress has been previously reported for cement paste [37]. This paper is partly directed at investigating for the first time the stress dependence of the permittivity of nickel-coated carbon fiber, with inclusion of the comparison of the behavior with and without the nickel coating.

The dependence of the permittivity on damage (not addressed in this work) enables capacitance-based damage self-sensing. Although this effect has not been previously reported for carbon fibers, capacitance-based damage self-sensing has been reported for a continuous carbon fiber polymer-matrix composite [38].

The piezoresistive behavior refers to the change of the electrical resistivity with stress/strain and is useful for stress/strain sensing through resistance measurement, i.e., resistance-based self-sensing. Negative piezoresistivity (the phenomenon in which the resistivity decreases with increasing strain) in continuous carbon fiber has been previously reported, with the stress-dependent gage factor ranging from −390 to −1830 [36]. The resistivity is central to conduction applications, so information on the effect of stress on the resistivity is useful, whether the piezoresistivity is positive or negative. This paper is partly directed at investigating the piezoresistive behavior of metal-coated carbon fiber for the first time, with inclusion of the comparison of the behavior with and without the metal coating.

Prior work on carbon fiber stress/strain self-sensing is limited to resistance-based self-sensing [39]. This work provides for the first time capacitance-based carbon fiber stress/strain self-sensing.

It should be emphasized that this paper is aimed at comparing the permittivity, piezoelectricity and piezoresistivity of the metal-coated carbon fiber and the corresponding uncoated carbon fiber, so as to understand the role of the metal coating. The metal coating on a carbon fiber differs in geometry from the monolithic metals, since its thickness is very small compared to the diameter of the fiber. The dimensional constraint of the thickness of the coating may cause preferred orientation of the grains of the metal. In contrast, for a monolithic metal, there tends to be relatively little preferred orientation. Therefore, this paper is also aimed at comparing the behavior of the metal-coated carbon fiber with that of the corresponding monolithic metal.

## 2. Basic concepts

### 2.1. Electric permittivity

The complex permittivity has real and imaginary parts, as illustrated in Fig. 1 [30]. In this paper, unless noted otherwise, the permittivity refers to the real part. It was commonly considered that a material of substantial electrical conductivity cannot have substantial permittivity (real part), due to the large magnitude of the imaginary part that is associated with the conductivity. The notion that the real part is small for a conductive material, so that the dielectric behavior of a conductive material can be neglected, was accepted without any measured value of the real part. However, the real part has recently been measured for highly conductive materials, including metals (such as steels, aluminum and copper) [31–33], continuous carbon fibers [34,35,38], continuous carbon fiber polymer-matrix composite [37] and discontinuous carbons (such as activated carbon, carbon black, natural graphite, exfoliated graphite, graphite oxide and reduced graphite oxide) [41–46]. For example, the measured value is $12230 \pm 990$ (2 kHz) for Teijin's Tenax HTS45 polyacrylonitrile (PAN) based carbon fiber with DC electrical resistivity $1.52 \times 10^{-5}$ Ω.m [35]. Based on the resistivity $\rho$, the imaginary part $\kappa$" (negative) of the relative permittivity (the part due to conduction loss only) is given by the equation [40].

$$- \kappa'' = 1/(\rho\, 2\pi\, \nu\, \varepsilon_o), \quad (1)$$

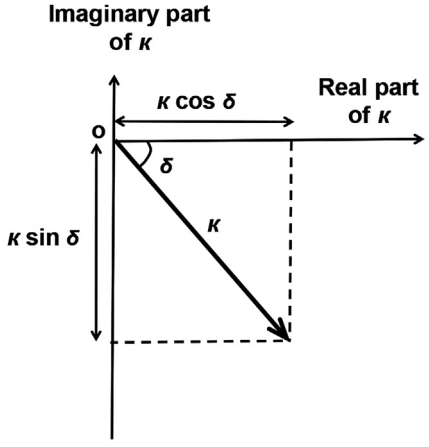


**Fig. 1.** Complex plane of the relative permittivity $\kappa$, showing the imaginary part of $\kappa$ (often known as $\kappa$") versus the real part of $\kappa$ (often known as $\kappa'$). In this paper, unless noted otherwise, the relative permittivity refers to the real part [30].

where $\nu$ is the frequency in Hz and $\varepsilon_o$ is the permittivity of free space ($8.85 \times 10^{-12}$ F/m). Thus, for the HTS45 carbon fiber at 2 kHz, - $\kappa'' = 5.9 \times 10^{11}$, which is greater than the measured value of 12230 for the real part by 7 orders of magnitude. This means that the high value of the real part is consistent with the high loss (i.e., large value of the angle $\delta$ in Fig. 1) that is expected for a conductive material. Therefore, the notion that a highly conductive material must have a low value of the permittivity is incorrect.

The relative permittivity of the metals decreases with increasing conductivity of the metal, as shown by comparing stainless steel, low carbon steel, aluminum and copper, which are listed in order of increasing conductivity (i.e., in order of decreasing permittivity) [31–33]. The resistivity of monolithic nickel is $6.99 \times 10^{-6}$ Ω.cm at 20 °C [46]. This value is higher than that of aluminum but lower than that of low carbon steel. Thus, one may expect that the relative permittivity of monolithic nickel is also intermediate between those of aluminum and low carbon steel.

### 2.2. Piezoelectricity

The change in polarization $\Delta P$ due to a change in stress is given by Ref. [30].

$$\Delta P = (\kappa - 1)(\Delta Q/A) + (\Delta\kappa)(Q/A) + \Delta\kappa\,\Delta Q/A, \quad (2)$$

where $\Delta Q$ is the change in the stored charge in the capacitor due to the change in stress $\Delta\sigma$, $\Delta\kappa$ is the change in $\kappa$ due to the change in stress, $\kappa$ is the relative permittivity in the absence of the change in stress, $Q$ is the stored charge in the absence of the change in stress, and $A$ is the area of the capacitor. The first term on the right side of Eq. (2) describes the classical piezoelectric effect that is due to the change in $Q$; the second term describes the less classical piezoelectric effect that is due to the change in $\kappa$; the third term describes the still less classical piezoelectric effect that is due to both the change in $\kappa$ and the change in $Q$. Thus, the polarization changes in response to both the change in $Q$ and the change in $\kappa$. The piezoelectric coupling coefficient $d$ (i.e., $d_{33}$) is given by

$$d = \Delta P/\Delta\sigma. \quad (3)$$

If the piezoelectric effect were solely and classically due to the change in $Q$ (i.e., the first term on the right side of Eq. (2)), $d$ is given by Ref. [30].

$$d = (\kappa - 1)\,\varepsilon_o\,\Delta E/\Delta\sigma, \quad (4)$$

where $\Delta E$ is the change in electric field due to the change in stress $\Delta\sigma$, as given by the slope of the initial linear part of the curve of $\Delta E$ vs. $\Delta\sigma$.

If the piezoelectric effect were solely due to the change in $\kappa$ (i.e., the second term on the right side of Eq. (2)),

$$d = (\Delta\kappa)(Q/A)\,/\,\Delta\sigma = (\Delta\kappa/\Delta\sigma)\,\varepsilon_o E, \quad (5)$$

where $E$ is the electric field in the absence of the change in stress, and $\Delta\kappa$ is the change in $\kappa$ due to the change in stress $\Delta\sigma$, as given by the slope of the initial linear part of the curve of $\Delta\kappa$ vs. $\Delta\sigma$.

If the piezoelectric effect were solely due to the last term on the right side of Eq. (2),

$$d = (\Delta\kappa/\Delta\sigma)\,\varepsilon_o\,\Delta E, \quad (6)$$

where $\Delta E$ is the change in electric field due to the change in stress $\Delta\sigma$.

### 2.3. Piezoresistivity

The fractional change in resistance ($\delta R/R$) relates to the fractional change in resistivity ($\delta\rho/\rho$), the longitudinal strain ($\delta\ell/\ell$) and the Poisson's ratio ($\nu$) according to the equation [30].

$$\delta R/R = \delta\rho/\rho + (\delta\ell/\ell)(1 + 2\nu), \quad (7)$$

for the case in which the material is isotropic in the two transverse directions, i.e., $\nu_{12} = \nu_{13}$. This case applies to the carbon fiber. For carbon fiber, $\nu = 0.27$ [47]. For nickel, $\nu = 0.31$ [48]. The gage factor, which is defined as the fractional change in resistance per unit strain, is a commonly used description of the extent of piezoresistivity. For a strain sensor that is not piezoresitive, but provides strain sensing due to the effect of the dimensional changes alone on the resistance, the gage factor is $1 + 2\nu$. The gage factor can be calculated based on Eq. (7), with the strain obtained by dividing the measured stress by the known elastic modulus.

## 3. Experimental methods

### 3.1. Materials

The nickel-coated continuous PAN-based carbon fiber is Tenax-J HTS40 A23 1420tex, with 12,000 fibers per tow, 1.3% sizing based on polyurethane resin, fiber diameter 7.5 μm (nickel coating thickness 0.25 μm, core carbon fiber diameter 7.0 μm), linear mass density 1420 tex, density 2.70 g/cm$^3$, electrical resistivity $7.5 \times 10^{-7}$ Ω.m, tensile modulus 215 GPa, tensile strength 2750 MPa, and tensile ductility 1.2% [49,50]. The fiber is provided by Teijin Limited. The nickel coating is deposited by the manufacturer on the carbon fiber by electroplating. The details of the electroplating process are proprietary. However, the process is likely conventional.

The corresponding uncoated continuous PAN-based carbon fiber that corresponds to the core carbon fiber of the nickel-coated carbon fiber is Tenax-E HTS45 E23 12K 800tex, with 12,000 fibers per tow, 1.3% sizing based on epoxy resin, fiber diameter 7.0 μm, linear mass density 800 tex, density 1.77 g/cm$^3$, electrical resistivity $1.6 \times 10^{-3}$ Ω.cm, tensile modulus 240 GPa, tensile strength 4500 MPa, and tensile ductility 1.9% [50–52]. The fiber is provided by Teijin Limited. This uncoated fiber is a high-strength standard-modulus aerospace grade carbon fiber. It is identical to that for which the relative permittivity of 12230 (2 kHz) was previously reported [35].

Compared to the uncoated carbon fiber, the nickel-coated carbon fiber exhibits lower modulus, lower strength, lower ductility, and, obviously, higher density and lower resistivity. There is no twist in either type of fiber. The nickel-coated carbon fiber is silvery grey in color whereas the uncoated carbon fiber is black. The nickel coating is uniformly distributed on the surface of the carbon fiber, as shown by scanning electron microscopy in prior work [53].

The Rule of Mixtures for the density $\varphi_{Ni\text{-}C}$ of the nickel-coated carbon fiber gives

$$\varphi_{Ni\text{-}C} = v_c\,\varphi_c + v_{Ni}\,\varphi_{Ni}, \quad (8)$$

where $\varphi_c$ and $\varphi_{Ni}$ are the densities of carbon and nickel, respectively, and $v_c$ and $v_{Ni}$ are the volume fractions of carbon and nickel, respectively. According to the above density values provided by the manufacturer, $\varphi_c = 1.770 \pm 0.005$ g/cm$^3$ and $\varphi_{Ni\text{-}C} = 2.700 \pm 0.005$ g/cm$^3$. The literature value for the density of nickel is $\varphi_{Ni} = 8.908 \pm 0.001$ g/cm$^3$ [54]. Note that

$$v_c + v_{Ni} = 1. \quad (9)$$

Based on Eqs. (8) and (9), $v_c = 0.870 \pm 0.002$, which is close to the geometric value of $v_c = 0.871 \pm 0.026$ calculated based on the nickel coating thickness ($0.250 \pm 0.005$ μm) and carbon fiber core diameter ($7.00 \pm 0.05$ μm). Between these two values of $v_c$, the value of $0.870 \pm 0.002$ is more accurate, so it is used in the remainder of this paper.

For the sake of comparison with nickel-coated carbon fiber, nickel wire is studied in terms of the permittivity and conductivity. The nickel is the nickel 200 alloy (99.6% commercially pure nickel). The 34-gauge wire has diameter 0.0063 in (0.160 mm) and linear resistance 1.511 Ω/ft (corresponding to resistivity $10 \times 10^{-8}$ Ω.m) at 20 °C, as supplied by TEMCo (Part No. RW0229).

### 3.2. Capacitance and permittivity measurement method

The method of permittivity measurement is the same as that of our prior work [35]. It involves a dielectric film between the specimen and each electrode (Fig. 2). The method also involves the decoupling of the interfacial capacitance from the volumetric capacitance, as explained below. In this context, the interface is that between the specimen and electrode, including the dielectric film. The specimen is a rectangular strip, with the long direction along the direction of capacitance measurement.

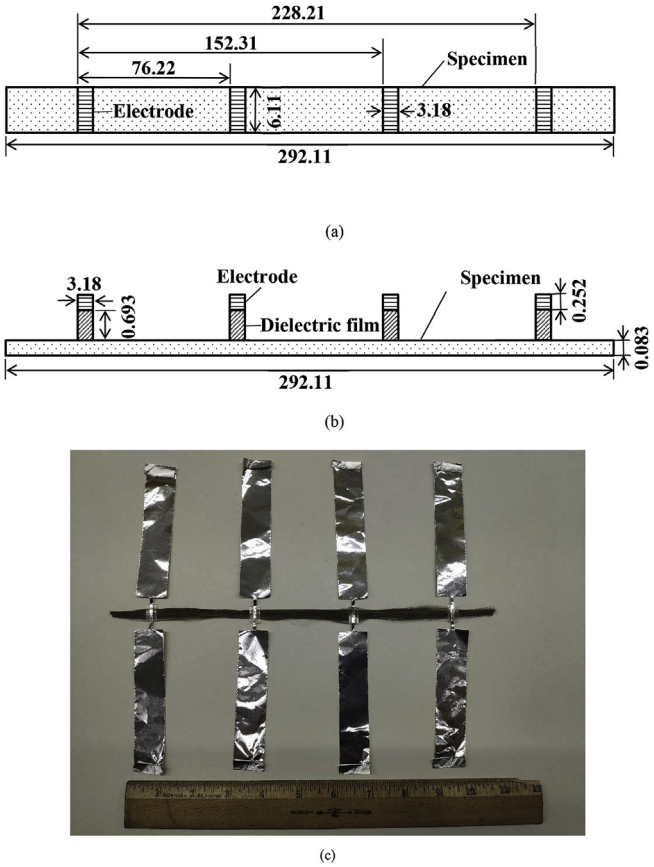


**Fig. 2.** Configuration for electric permittivity measurement. (a) Schematic illustration (top view), with the dimensions shown in mm for the nickel-coated carbon fiber. (b) Schematic illustration (side view), with the dimensions shown in mm for the nickel-coated carbon fiber, showing a dielectric film between each electrode and the specimen. The vertical axis is expanded, with the scale different from that of the horizontal axis. (c) Photograph of the nickel-coated carbon fiber tow (horizontal) with four aluminum foil electrodes and including a ruler with main divisions in inches. Each electrode (3.18 mm wide) is much narrower for the region above the specimen than the regions away from the specimen. (A colour version of this figure can be viewed online.)

For decoupling the interfacial capacitance from the volumetric capacitance, four electrodes in the form of aluminum foil are positioned on the top surface of the specimen at four points (essentially equally spaced at a distance of ~76 mm, with the exact value measured for each specimen) along the length of the specimen (Fig. 2). Each electrode is adhered to the top surface of the specimen by using multiple layers of double-sided adhesive tape (thickness 0.077 mm per layer; 11 layers, 9 layers and 6 layers for the nickel wire, nickel-coated carbon fiber and uncoated carbon fiber, respectively, with the required number of layers increasing with decreasing resistance of the material being tested), which serves as the dielectric film. Each electrode is 3.18 mm wide in the direction of the length of the specimen, such that it extends all the way along the 6.11-mm width of the specimen. By using different pairs of electrodes (the 1st and 2nd, the 1st and 3rd, and the 1st and 4th), measurement of the capacitance is conducted over distances of $L$ (~76 mm), $2L$ (~152 mm) and $3L$ (~228 mm), with the exact values measured for each specimen.

The capacitance is measured using an LCR meter (Instek LCR-816 High Precision LCR Meter). The frequency is 2.000 kHz, because this is the highest frequency provided by the meter and a frequency in the kHz range is commonly available and widely used. The error in the capacitance measurement is ±0.0005 pF. The capacitance reported is that for the equivalent circuit of capacitance and resistance in series. This circuit model is intended to indicate the setting used in the meter, rather than the method of analysis. The voltage (0.300, 0.600 or 0.900 V) is adjusted so that the electric field (3.95 V/m) is the same for the different distances between the chosen electrodes of a pair.

For measurement using each pair of electrodes, the two interfacial capacitances (for the two specimen-electrode interfaces) and the specimen volumetric capacitance are three capacitors in series electrically. Hence, the measured capacitance $C_m$ is given by

$$1/C_m = 1/C + 2/C_i, \tag{10}$$

where $C$ is the specimen volumetric capacitance, and $C_i$ is the interfacial capacitance for one interface. The $C$ relates to $\kappa$ of the specimen by the equation

$$C = \varepsilon_o \kappa A/l, \tag{11}$$

where $\varepsilon_o$ is the permittivity of free space, $A$ is the area of the specimen in the plane perpendicular to the direction of capacitance measurement, and $l$ is the length of the specimen between the two electrodes in the direction of the capacitance measurement (i.e., $L$, $2L$ or $3L$). Combining Eqs. (10) and (11) gives

$$1/C_m = l/(\varepsilon_o \kappa A) + 2/C_i. \tag{12}$$

Based on Eq. (12), a plot of $1/C_m$ vs. $l$ gives a line of slope equal to $1/(\varepsilon_o \kappa A)$. Hence, from the slope, $\kappa$ is obtained.

### 3.3. Electric field output measurement method

The voltage output is measured using the same specimen configuration as Fig. 2, except that the dielectric film is replaced by silver paint. The DC voltage is measured using a precision digital multimeter (Keithley Model 2002). For the relevant voltage range (within 200 mV), the resolution is 1 nV and the input resistance exceeds 100 GΩ [55]. The electric field is the voltage divided by the distance between the proximate edges of the electrodes.

### 3.4. Resistivity measurement method

The resistivity is measured using the same specimen configuration as Fig. 2, except that the dielectric film is replaced by silver paint. The same specimens are used first for permittivity measurement and then for conductivity measurement. By using different pairs of electrodes (the 1st and 2nd, the 1st and 3rd, and the 1st and 4th), measurement of the resistance is conducted over distances of $L$ (~76 mm), $2L$ (~152 mm) and $3L$ (~228 mm), with the exact values measured for each specimen.

For measurement using each pair of electrodes, the two interfacial resistances and the specimen volumetric resistance are three resistors in series electrically. Hence, the measured resistance $R_m$ is given by

$$R_m = R + 2R_i, \tag{13}$$

where $R$ is the specimen volumetric resistance, and $R_i$ is the interfacial resistance for one interface. The $R$ relates to the resistivity $\rho$ of the specimen by the equation

$$R = \rho l/A, \tag{14}$$

where $A$ is the area of the specimen in the plane perpendicular to the direction of resistance measurement, and $l$ is the length of the specimen between the two electrodes (i.e., $L$, $2L$ or $3L$).

Combining Eqs. (13) and (14) gives

$$R_m = \rho l/A + 2R_i, \tag{15}$$

Based on Eq. (15), a plot of $R_m$ vs. $l$ gives a line of slope equal to $\rho/A$. Hence, from the slope, $\rho$ is obtained.

The DC resistance is measured using a precision digital multimeter (Keithley Model 2002) operating in the two-wire mode. For the range of resistance of this work, the resolution is 100 nΩ and the current provided by the meter is 7.2 mA [55].

### 3.5. Mechanical testing method

The mechanical testing system is stepper motor-driven (Mark-10 ESM303, Mark-10 Corp., Copiague, NY), providing force up to 1.5 kN. The force is increased at the rate 90 N/min. The tensile stress is given by the force divided by the cross-sectional area of the specimen. In case of carbon fiber specimens, the cross-sectional area of the specimen is the cross-sectional area of 12,000 fibers.

The specimen is a single tow/wire, with the tow/wire axis along the direction of capacitance/resistance measurement. The specimen is adhered at its two ends by using epoxy adhesive on a cardboard that is in the shape of a picture frame (Fig. 2). The two sides of the picture frame parallel to the specimen are cut just before the start of tensile testing, which is performed along the tow axis.

The tensile modulus determined in our prior work [36] on the uncoated carbon fiber up to a stress of 110 MPa and a strain of 0.046% is (239.2 ± 0.6) GPa. This value is consistent with the value of 240 GPa provided by the manufacturer [50]. The consistency supports the reliability of the mechanical testing method of this work.

## 4. Results and discussion

### 4.1. In the absence of stress

For both nickel-coated and uncoated carbon fibers and for the nickel wire, the plot of $1/C_m$ vs. distance $l$ according to Eq. (12) and the plot of $R_m$ vs. distance $l$ according to Eq. (15) are highly linear. Figs. 3–5 give the plots for the nickel-coated carbon fiber, uncoated carbon fiber and nickel wire, respectively. The error in the relative permittivity $\kappa$ or resistivity $\rho$ is obtained by considering the range of values of the slope.

Table 1 shows that $\kappa$ is much higher while $\rho$ is much lower for the nickel-coated carbon fiber than the uncoated carbon fiber. In other words, the presence of the nickel coating greatly increases $\kappa$ and greatly decreases $\rho$. The latter is well-known, but the former has not been previously reported.

The resistivity value of $(1.52 \pm 0.03) \times 10^{-7}$ Ω.m for the nickel-coated carbon fiber is lower than the manufacturer-provided value of $7.5 \times 10^{-7}$ Ω.m [49–51]. On the other hand, the resistivity value of $(1.52 \pm 0.04) \times 10^{-5}$ Ω.m for the uncoated carbon fiber is close to the manufacturer-provided value of $1.6 \times 10^{-5}$ Ω.m [52].

A nickel-coated carbon fiber consists of the nickel coating and the carbon fiber core that are electrically in parallel. Thus, the relative permittivity $\kappa$ of the nickel-coated carbon fiber is given by

$$\kappa = \kappa_C v_C + \kappa_{Ni} v_{Ni}, \tag{16}$$

where $v_C$ and $v_{Ni}$ are the volume fractions of carbon and nickel,

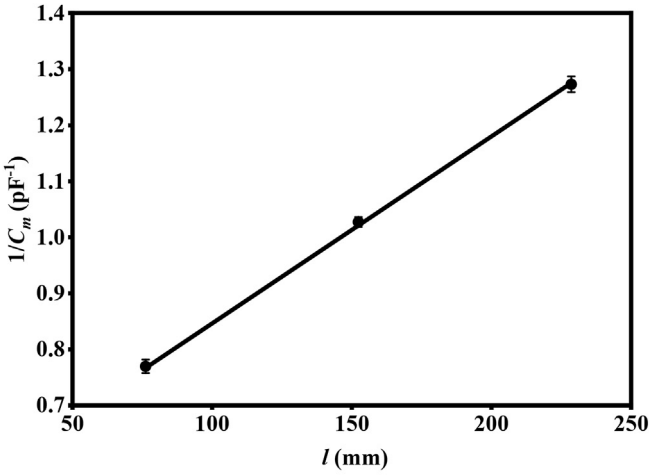


(a)

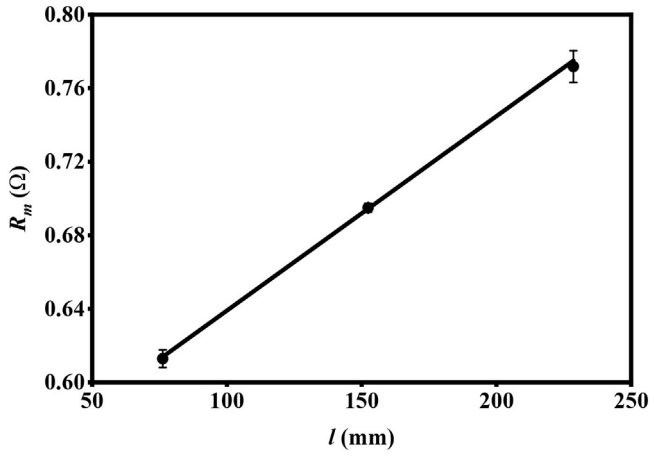


(b)

**Fig. 3.** Results for nickel-coated carbon fiber in the absence of stress. (a) Plot of $1/C_m$ vs. distance $l$ according to Eq. (12). (b) Plot of $R_m$ vs. distance $l$ according to Eq. (15).

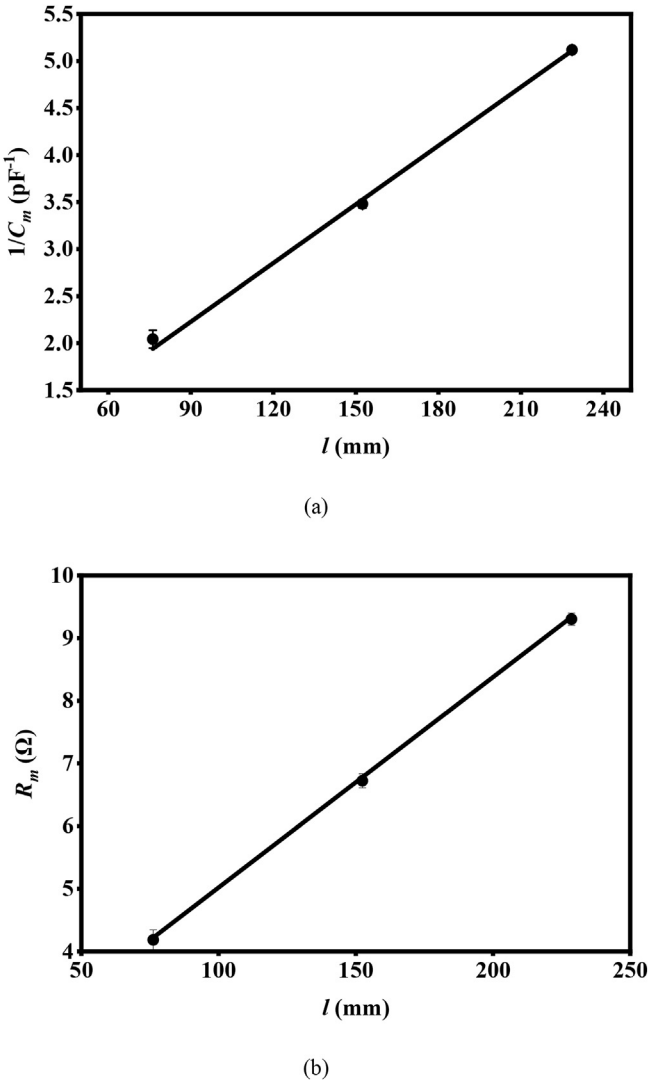


**Fig. 4.** Results for uncoated carbon fiber in the absence of stress. (a) Plot of $1/C_m$ vs. distance $l$ according to Eq. (12). (b) Plot of $R_m$ vs. distance $l$ according to Eq. (15).

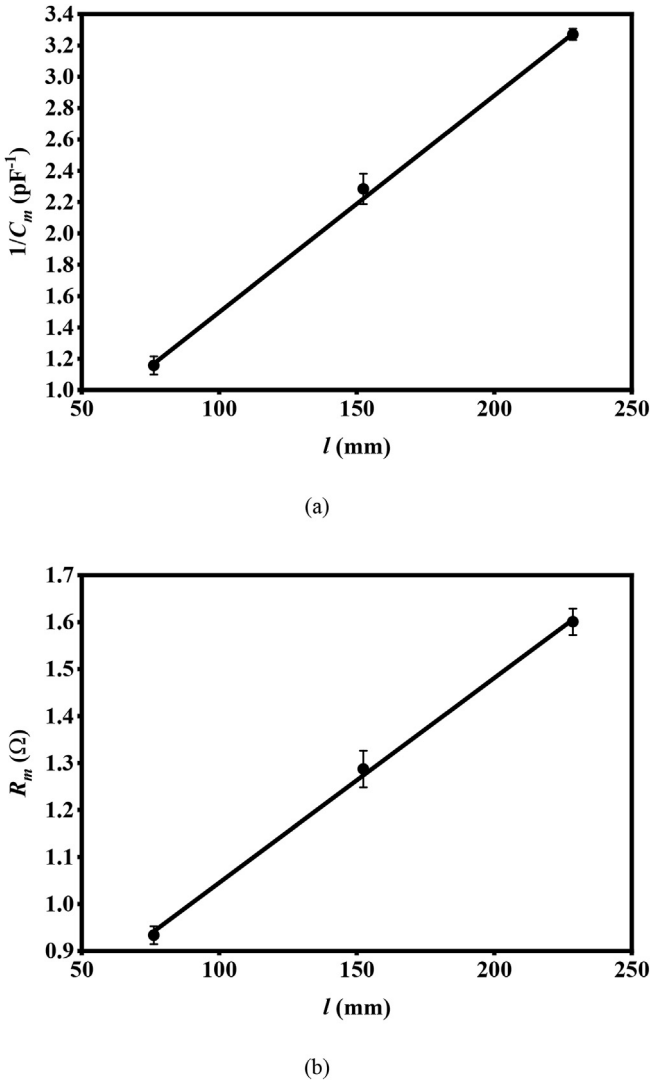


**Fig. 5.** Results for nickel wire in the absence of stress. (a) Plot of $1/C_m$ vs. distance $l$ according to Eq. (12). (b) Plot of $R_m$ vs. distance $l$ according to Eq. (15).

respectively, and $\kappa_C$ and $\kappa_{Ni}$ are the relative permittivity values of carbon and nickel, respectively From Table 1, $\kappa_C = 12233 \pm 994$ and $\kappa = 63246 \pm 1305$. Hence, based on Eq. (16) and $v_c = 0.870 \pm 0.002$, one obtains $\kappa_{Ni} = 404640 \pm 3749$. Thus, the relative permittivity of the nickel coating is much higher than that of the core carbon fiber, and is responsible for the large increase in relative permittivity of the fiber due to the presence of the nickel coating.

The relative permittivity of the nickel wire, as obtained in this work from the slope of the highly linear plot of $1/C_m$ vs. distance $l$ according to Eq. (12), is $405307 \pm 2597$, which is essentially the same as the abovementioned $\kappa_{Ni}$ value for the nickel coating on the carbon fiber. This consistency supports the correctness of the method used in this work for determining the permittivity of the nickel coating.

The relative permittivity values of aluminum and low carbon steel are $5.5 \times 10^4$ [32] and $1.1 \times 10^6$ [31], respectively. The abovementioned value of nickel ($4.1 \times 10^5$) is between the values of aluminum and low carbon steel, as expected (Sec. 2.1).

Similarly, since the nickel coating and the core carbon fiber are in parallel, the conductivity $\sigma$ of the nickel-coated carbon fiber is given by

$$\sigma = \sigma_C v_C + \sigma_{Ni} v_{Ni}, \quad (17)$$

where $\sigma_C$ and $\sigma_{Ni}$ are the conductivity values of carbon and nickel, respectively. From Table 1, $\sigma_C = 1/[(1.52 \pm 0.04) \times 10^{-5}\,\Omega.m]$ and $\sigma = 1/[(1.52 \pm 0.03) \times 10^{-7}\,\Omega.m]$. Hence, based on Eq. (17) and $v_c = 0.870 \pm 0.002$, one obtains the nickel resistivity $\rho_{Ni} = (1.99 \pm 0.09) \times 10^{-8}\,\Omega.m$ (Table 1). The resistivity of the nickel wire, as obtained in this work from the slope of the highly linear plot of $R_m$ vs. distance $l$ according to Eq. (15), is $(8.81 \pm 0.06) \times 10^{-8}\,\Omega.m$, which is close to the value of $10 \times 10^{-8}\,\Omega.m$ calculated based on the manufacturer-provided linear resistance of this wire, and is also close to the literature value of $6.99 \times 10^{-8}\,\Omega.m$ for nickel [46]. Hence, the resistivity of the nickel coating along the fiber axis is lower than that of monolithic nickel, in spite of the similarity in the permittivity. This is because electrical conduction is more sensitive to the structure than polarization, as expected from the fact that the extent of electron movement is greater in conduction than polarization. The greater degree of preferred crystallographic orientation in the nickel coating probably enhances the conductivity without affecting the permittivity. The occurrence of preferred orientation in nickel films obtained by electroplating has been previously

**Table 1**
Relative permittivity (2 kHz) and electrical resistivity (DC) of nickel-coated and uncoated carbon fibers and nickel wire, all in the absence of stress. The values for the nickel coating are also shown, as obtained by calculation using the Rule of Mixtures and the values for the nickel-coated and uncoated fibers.

| | Uncoated carbon fiber [35] | Nickel-coated carbon fiber | Nickel coating | Nickel wire |
|---|---|---|---|---|
| Relative permittivity | $12233 \pm 994$ | $63246 \pm 1305$ | $404640 \pm 3749$ | $405307 \pm 2597$ |
| Resistivity (Ω.m) | $(1.52 \pm 0.04) \times 10^{-5}$ | $(1.52 \pm 0.03) \times 10^{-7}$ | $(1.99 \pm 0.09) \times 10^{-8}$ | $(8.81 \pm 0.06) \times 10^{-8}$ |

reported [56–59].

The resistivity of monolithic copper is $(1.38 \pm 0.03) \times 10^{-8}$ Ω.m [33], as we measured using the method of this work. Hence, the resistivity of the nickel coating is higher than but close to that of monolithic copper.

### 4.2. In the presence of stress

Fig. 6 shows that the electric field output increases monotonically with increasing tensile stress for both uncoated carbon fiber and nickel-coated carbon fiber. The trend is the same for the nickel wire, though the fractional change in electric field due to the stress is relatively small for the nickel wire. The fractional change in electric field due to the stress is greater for the uncoated carbon fiber than the nickel-coated carbon fiber. This means that the presence of the nickel coating diminishes the piezoelectric behavior, due to the much stronger piezoelectric effect in the uncoated carbon fiber than nickel itself.

Fig. 7 shows that the relative permittivity increases with increasing stress for the uncoated carbon fiber, but decreases with increasing stress for the nickel-coated carbon fiber and the nickel wire. This means that the effect of stress on the permittivity of nickel-coated carbon fiber is mainly governed by the nickel coating. This is consistent with the fact that the permittivity of nickel-coated carbon fiber is dominated by that of the nickel coating (Sec. 4.1 and Table 1). For the same stress, the magnitude of the fractional change in relative permittivity due to the stress is greater for the uncoated carbon fiber than the nickel-coated carbon fiber, and is much lower for the nickel wire than uncoated or nickel-coated carbon fiber. The low magnitude of the fractional change in relative permittivity due to the stress for the nickel-coated carbon fiber is due to the weakness of this effect for the nickel itself.

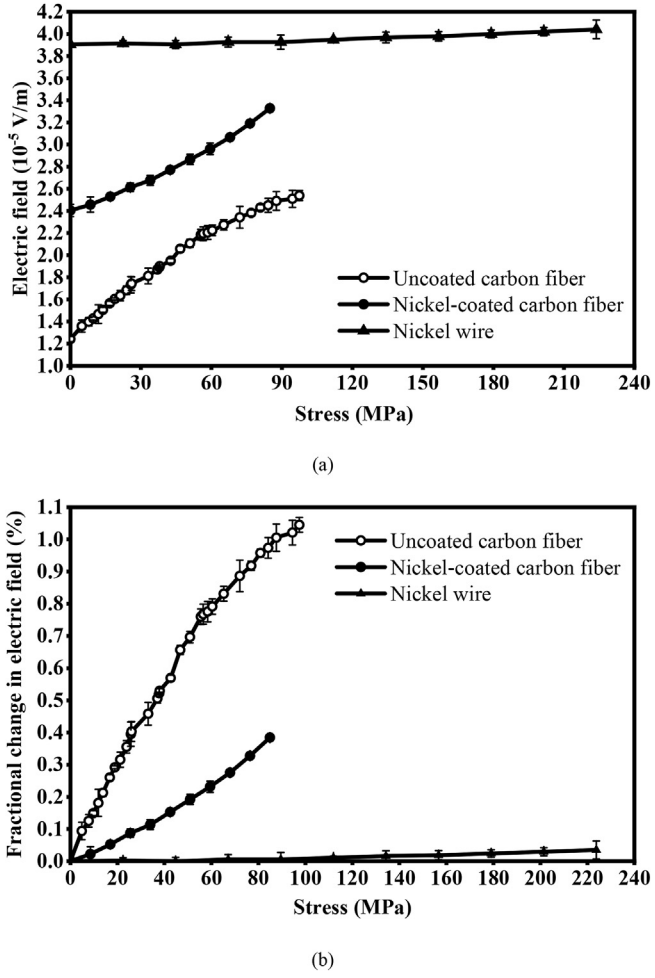


**Fig. 6.** Effect of tensile stress on the electric field output due to the direct piezoelectric effect. (a) Electric field. (b) Fractional change in electric field due to the stress.

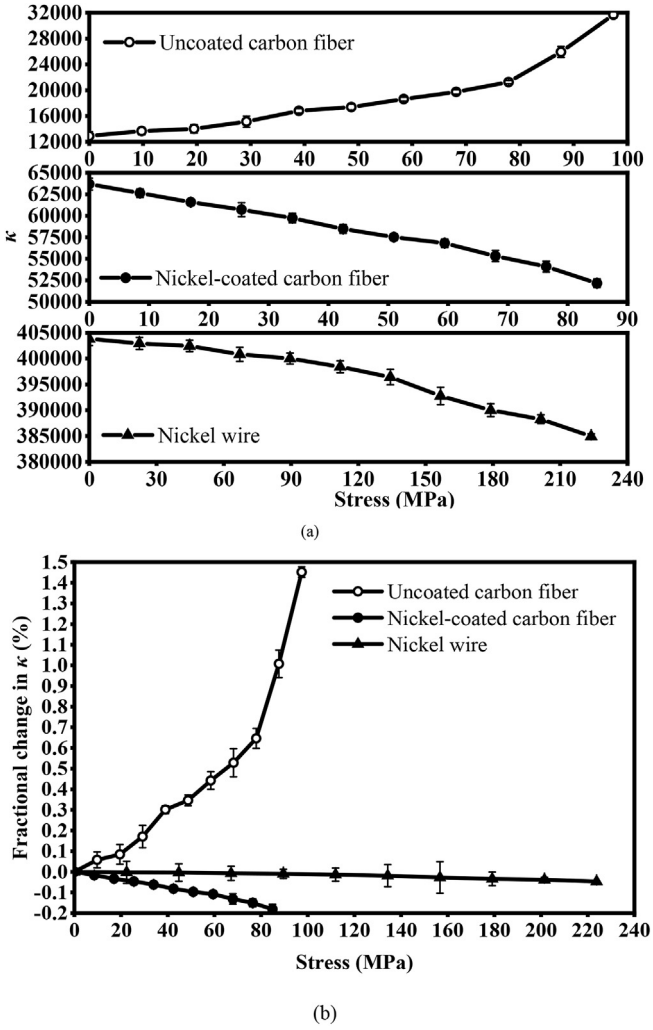


**Fig. 7.** Effect of tensile stress on the relative permittivity κ. (a) κ. (b) Fractional change in κ due to the stress.

**Table 2**
Piezoelectric coupling coefficient ($d_{33}$) and piezoresistive gage factor of uncoated carbon fiber, nickel-coated carbon fiber and nickel wire.

| | Uncoated carbon fiber [36] | Nickel-coated carbon fiber | Nickel wire |
|---|---|---|---|
| $d_{33}$ (pC/N), Eq. (4) [a] | $+(1.7 \pm 0.3) \times 10^{-8}$ | $+(5.6 \pm 0.2) \times 10^{-9}$ | $+(3.0 \pm 0.1) \times 10^{-9}$ |
| $d_{33}$ (pC/N), Eq. (5) [b] | $+(1.3 \pm 0.2) \times 10^{-8}$ | $-(2.6 \pm 0.4) \times 10^{-14}$ | $-(4.2 \pm 0.4) \times 10^{-14}$ |
| $d_{33}$ (pC/N), Eq. (6) [b] | $+(9.3 \pm 0.7) \times 10^{-9}$ | $-(9.8 \pm 0.2) \times 10^{-15}$ | $-(1.5 \pm 0.3) \times 10^{-15}$ |
| Gage factor[c] | $-1830 \pm 47$ | $+1651 \pm 35$ | $+30 \pm 1$ |

[a] Obtained from the slope of the main linear region of the curve of the electric field vs. stress.
[b] Obtained from the slope of the main linear region of the curve of the relative permittivity vs. stress.
[c] Obtained from the slope of the main linear region of the curve of resistivity versus stress.

For any of the three types of material, the magnitude of $d_{33}$ obtained by using Eq. (4) is higher than that obtained by using Eq. (5) or (6). This means that the piezoelectricity mechanism corresponding to Eq. (4) dominates. As shown in Table 2, the magnitude of $d_{33}$ is similar for nickel-coated carbon fiber and nickel wire, and is greater for uncoated carbon fiber than nickel-coated carbon fiber. However, all values are small compared to those of well-known piezoelectric materials, indicating that the piezoelectric effect is weak.

For the uncoated carbon fiber, $d_{33}$ is positive, whether it is obtained by using Eq. (4) and (5) or (6). In contrast, for the nickel-coated carbon fiber and nickel wire, $d_{33}$ is positive if it is obtained by using Eq. (4), but is negative if it is obtained by using Eq. (5) or (6). The negative values of $d_{33}$ are due to the permittivity decreasing with increasing stress.

The nickel-coated carbon fiber and nickel wire are similar in the piezoelectric behavior, whereas the uncoated carbon fiber behaves differently (Table 2). This indicates that the nickel coating primarily governs the piezoelectric behavior of the nickel-coated carbon fiber.

Fig. 8 shows that the resistivity decreases with increasing tensile stress for the uncoated carbon fiber, but increases with increasing tensile stress for the nickel-coated carbon fiber and nickel wire. Hence, the piezoresistive behavior of nickel-coated carbon fiber is mainly governed by that of the nickel coating. This is consistent with the fact that the conductivity of nickel-coated carbon fiber is dominated by that of the nickel coating (Sec. 4.1 and Table 1). The observation that the piezoresistivity is weak and positive for nickel is expected from the metallic character of nickel. For the same stress, the magnitude of the fractional change in resistivity due to the stress is higher for the uncoated carbon fiber than the nickel-coated carbon fiber and is much lower for the nickel wire than uncoated or nickel-coated carbon fiber. Thus, the relatively low magnitude of the fractional change in resistivity due to the stress for the nickel-coated carbon fiber is due to the weakness of this effect in nickel itself.

Table 2 shows that the piezoresistive gage factor is negative for the uncoated carbon fiber and positive for the nickel-coated carbon fiber and nickel wire. The magnitude of the gage factor is comparable for the uncoated and nickel-coated carbon fibers, but is much smaller for the nickel wire. Thus, both uncoated and nickel-coated carbon fibers can provide resistance-based stress self-sensing.

As noted in our prior work [38], the negative gage factor for the uncoated carbon fiber is due to the increase in the degree of carbon layer preferred orientation along the fiber axis as the tensile stress increases. The positive gage factor of the nickel-coated carbon fiber is in line with the positive gage factor of the nickel wire. It indicates the dominance of the nickel coating in governing the piezoresistivity of the nickel-coated carbon fiber. The large positive gage factor of the nickel-coated carbon fiber cannot be explained in terms of the Rule of Mixtures and the gage factor values of the uncoated carbon fiber and nickel wire. This implies that the gage factor of the nickel coating (not determined) differs considerably from that of the nickel wire. This difference is consistent with the difference in resistivity between the nickel coating and the nickel wire (Sec. 4.1). More work is needed to identify the difference in structure between the nickel coating and the nickel wire.

The nickel coating changes the stress dependence of the permittivity from positive to negative and changes the piezoresistivity from negative to positive. This suggests that positive stress dependence of the relative permittivity correlates with negative piezoresistivity, and negative stress dependence of the permittivity correlates with positive piezoresistivity. In other words, it suggests that higher permittivity correlates with lower resistivity. This correlation is consistent with the previous report that the relative permittivity is $4960 \pm 662$ and $3960 \pm 450$ (also 2 kHz) for Thornel P-100 (more graphitic, lower resistivity) and Thornel P-25 fibers (less graphitic, higher resistivity), respectively [34]. This correlation is due to the ease of free electron movement promoting both conduction and polarization. Afterall, the real and imaginary parts of the permittivity are not independent of one another, as indicated by the Kramers-Kronig relationship [60]. This relationship requires data over a wide range of frequencies, ideally from 0 to $\infty$, so the feasibility of its implementation is limited.

The change of the relative permittivity with stress is useful for capacitance-based stress self-sensing, whereas the change of the resistivity with stress is useful for resistance-based stress self-sensing. Capacitance-based sensing is advantageous over resistance-based sensing in that the electrical contacts do not need to be in intimate electrical contact with the specimen. In this work, the electrical contacts for capacitance measurement are in the form of aluminum foil attached to the specimen using adhesive tape, whereas those for resistance measurement are in the form of aluminum foil attached to the specimen using silver paint. In practical structural implementation of the technology, the fiber composite structure may be covered with a layer of paint, which can serve as the dielectric film. Hence, the removal of the paint is not necessary for capacitance measurement, but is necessary for resistance measurement.

## 5. Conclusion

This paper unprecedentedly reports the effect of metal (nickel) coating on the electric permittivity, piezoelectricity and piezoresistivity of carbon fiber. In addition, it reports the effect of stress on the permittivity of carbon fiber with and without the nickel coating. Nickel-coated carbon fibers are widely used for electrical, electrochemical, electrothermal and electromagnetic applications. The electric permittivity is relevant to all these applications. In addition, the stress-dependent permittivity enables capacitance-based stress self-sensing, whereas the piezoresistivity enables resistance-based stress self-sensing.

This paper reports for the first time the permittivity of a metal-coated carbon fiber. The experimental methods involve the decoupling of the interfacial and volumetric contributions to the capacitance or resistance. The interface refers to that between the

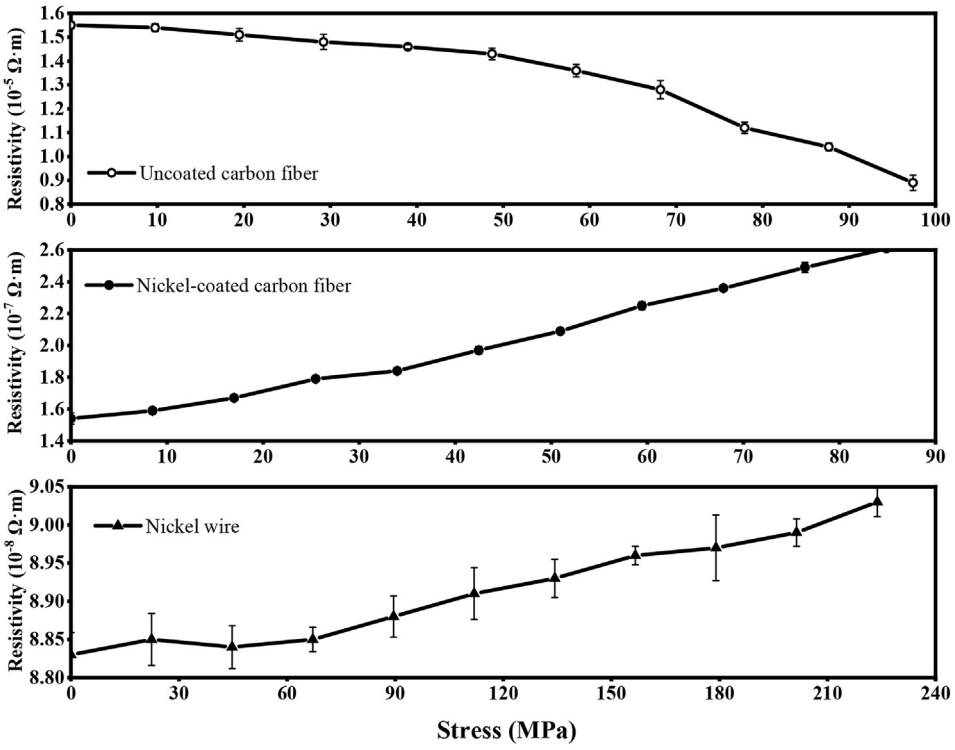


(a)

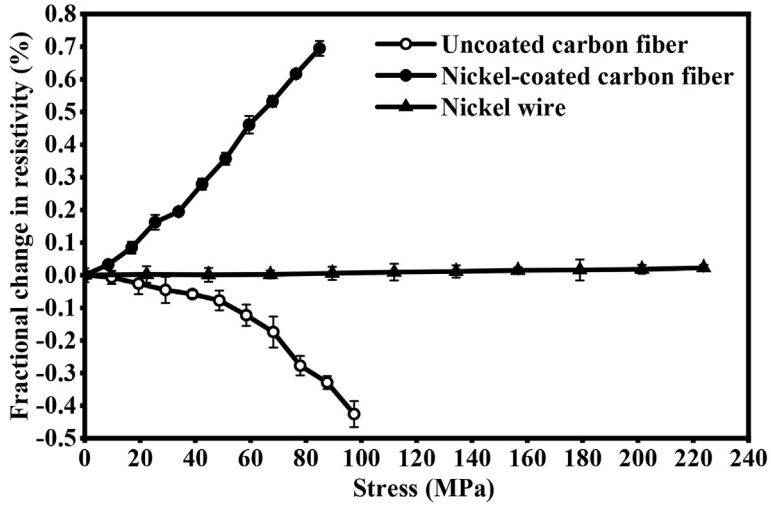


(b)

**Fig. 8.** Effect of tensile stress on the resistivity. (a) Resistivity. (b) Fractional change in resistivity due to the stress.

specimen and an electrode.

Both the permittivity and conductivity of continuous carbon fiber are greatly increased by nickel coating. For a high-strength standard-modulus PAN-based carbon fiber of diameter 7 μm, a nickel coating of thickness 0.25 μm, as obtained by electroplating, increases the relative permittivity (2 kHz) by 420% from 12,200 to 63,200, while the DC resistivity is decreased by two orders of magnitude from $1.5 \times 10^{-5}$ to $1.5 \times 10^{-7}$ Ω.m. The increases in both permittivity and conductivity stem from the enhanced electron movement due to the nickel coating.

The relative permittivity of the nickel coating, as calculated based on the Rule of Mixtures, is 404,600, which is similar to the value of 405,300 for nickel wire (diameter 160 μm). The resistivity of the nickel coating, as calculated based on the Rule of Mixtures, is $2.0 \times 10^{-8}$ Ω.m, which is lower than the value of $8.8 \times 10^{-8}$ Ω.m for the nickel wire, probably because of the higher degree of preferred crystallographic orientation in the nickel coating. The nickel structure affects the conduction (conductivity) more than the polarization (permittivity).

The piezoelectric and piezoresistive effects are diminished by the presence of the nickel coating, which dominates over the carbon in governing these effects. The nickel coating changes the stress dependence of the permittivity (for capacitance-based self-sensing) from positive to negative and changes the piezoresistivity (for resistance-based self-sensing) from negative (gage factor −1830) to positive (gage factor +1650). This is due to the

correlation of high permittivity with low resistivity. The piezoelectricity of the nickel-coated carbon fiber and nickel wire are similar, but the piezoresistivity is weak for the latter (gage factor +30).

## References


[1] N. Ning, S. Liu, Q. Shao, S. Yan, H. Zou, L. Zhang, M. Tian, Conductivity stability and its relationship with the filler network structure of elastomer composites with combined fibrous/layered nickel-coated fillers, RSC Adv. 4 (61) (2014) 32482–32489.

[2] S.J. Lim, J.G. Lee, S.H. Hur, W.N. Kim, Effects of MWCNT and nickel-coated carbon fiber on the electrical and morphological properties of polypropylene and polyamide 6 blends, Macromol. Res. 22 (6) (2014) 632–638.

[3] D. Whitworth, M. Miles, D. Fullwood, G. Hansen, B. Strong, Electrical properties of polythylene with nickel nanostrands and nickel coated carbon fiber reinforcement, Int SAMPE Technical Conf 42 (2010) a79/1-a79/8.

[4] L. Bertolini, F. Bolzoni, T. Pastore, P. Pedeferri, Effectiveness of a conductive cementitious mortar anode for cathodic protection of steel in concrete, Cement Concr. Res. 34 (4) (2004) 681–694.

[5] T. Kim, D.D.L. Chung, Mats and fabrics for electromagnetic interference shielding, J. Mater. Eng. Perform. 15 (3) (2006) 295–298.

[6] X. Shui, D.D.L. Chung, Nickel filament polymer-matrix composites with low surface impedance and high electromagnetic interference shielding effectiveness, J. Electron. Mater. 26 (8) (1997) 928–934.

[7] X. Shui, D.D.L. Chung, 0.4 μm diameter nickel filament silicone-matrix resilient composites for electromagnetic interference shielding, J. Electron. Packag. 119 (4) (1997) 236–238.

[8] S.H. Lee, J.Y. Kim, C.M. Koo, W.N. Kim, Effects of processing methods on the electrical conductivity, electromagnetic parameters, and EMI shielding effectiveness of polypropylene/nickel-coated carbon fibercomposites, Macromol. Res. 25 (9) (2017) 936–943.

[9] J.M. Kim, Y. Lee, M.G. Jang, C. Han, W.N. Kim, Electrical conductivity and EMI shielding effectiveness of polyurethane foam-conductive filler composites, J. Appl. Polym. Sci. 134 (5) (2017) (NA).

[10] X. Chen, X. Wang, L. Li, S. Qi, Preparation and microwave absorbing properties of nickel-coated carbon fiber with polyaniline via in situ polymerization, J. Mater. Sci. Mater. Electron. 27 (6) (2016) 5607–5612.

[11] W. Chen, J. Wang, T. Wang, J. Wang, B. Zhang, Electromagnetic interference shielding properties of nickel-coated carbon fiber veil/acid-functionalized MWCNTs/epoxy multiscale composites, J. Reinforc. Plast. Compos. 34 (13) (2015) 1029–1039.

[12] R. Wang, H. Yang, J. Wang, F. Li, The electromagnetic interference shielding of silicone rubber filled with nickel coated carbon fiber, Polym. Test. 38 (2014) 53–56.

[13] T.W. Yoo, Y.K. Lee, S.J. Lim, H.G. Yoon, W.N. Kim, Effects of hybrid fillers on the electromagnetic interference shielding effectiveness of polyamide 6/conductive filler composites, J. Mater. Sci. 49 (4) (2014) 1701–1708.

[14] S. Luo, Z. He, Ni-coated carbon fiber as cathode material for microbial fuel cells, Electrochim. Acta 222 (2016) 338–346.

[15] B. Pierozynski, L. Smoczynski, Electrochemical corrosion behavior of nickel-coated carbon fiber materials in various electrolytic media, J. Electrochem. Soc. 155 (8) (2008) C427–C436.

[16] T. Kim, D.D.L. Chung, Carbon fiber mats as resistive heating elements, Carbon 41 (12) (2003) 2436–2440.

[17] D.D.L. Chung, Self-heating structural materials, Smart Mater. Struct. 13 (3) (2004) 562–565.

[18] X. Hou, H. Chen, C. Xu, G. Liu, Y. Liu, Conductive nickel/carbon fiber composites prepared via an electroless plating route, J. Mater. Sci. Mater. Electron. 27 (6) (2016) 5686–5690.

[19] X. Shui, D.D.L. Chung, Magnetic properties of nickel filament polymer-matrix composites, J. Electron. Mater. 25 (6) (1996) 930–934.

[20] D.C. Stanier, J. Ciambella, S.S. Rahatekar, Fabrication and characterisation of short fibre reinforced elastomer composites for bending and twisting magnetic actuation, Composites, Part A 91 (Part 1) (2016) 168–176.

[21] K. Shiraishi, S. Inui, S. Ishii, Y. Matsumura, Y. Nishi, Tensile strength of Al/ABS-CFRP joint reinforced by nickel coated carbon fiber cloth, Mater. Trans. 55 (10) (2014) 1564–1567.

[22] S. Inui, K. Shiraishi, S. Ishii, A. Kasai, N. Miwa, M. Kanda, Y. Nishi, Polymer/metal joining with carbon fibers with high resistance to pull-out induced by huge friction force generated by extremely broad total interface area, Adv. Mater. Res. 922 (THERMEC 2013 Supplement) (2014), 270-273, 5.

[23] Y. Nishi, S. Ishii, S. Inui, A. Kasai, M.C. Faudree, Impact value of CFRP/Ti joint reinforced by nickel coated carbon fiber, Mater. Trans. 55 (2) (2014) 323–326.

[24] B. Pierozynski, T. Mikolajczyk, M. Turemko, Influence of nickel electrodeposition on tensile strength of carbon fiber tow material, Int J Electrochemical Sci 8 (11) (2013) 12273–12277.

[25] S. Kushwaha, K.K. Kar, P.S.G. Krishnan, S.K. Sharma, Preparation and characterization of nickel coated carbon fiber reinforced polycarbonate composites, J. Reinforc. Plast. Compos. 30 (14) (2011) 1185–1196.

[26] B. Pierozynski, Electrodeposition of nickel onto 12K carbon fibre tow in a continuous manner, Croat. Chem. Acta 85 (1) (2012) 1–8.

[27] Z. Hua, Y. Liu, G. Yao, L. Wang, J. Ma, L. Liang, Preparation and characterization of nickel-coated carbon fibers by electroplating, J. Mater. Eng. Perform. 21 (3) (2012) 324–330.

[28] S. Tzeng, F. Chang, Electrical resistivity of electroless nickel coated carbon fibers, Thin Solid Films 388 (1,2) (2001) 143–149.

[29] S. Tzeng, F. Chang, EMI shielding effectiveness of metal-coated carbon fiber-reinforced ABS composites, Mater. Sci. Eng., A A302 (2) (2001) 258–267.

[30] D.D.L. Chung, Functional Materials, World Sci Pub, 2010 (Chapter 3).

[31] D.D.L. Chung, K. Shi, Sensing the stress in steel by capacitance measurement, Sensor. Actuator. 274 (2018) 244–251.

[32] X. Xi, D.D.L. Chung, Capacitance-based nondestructive evaluation of aluminum, with measurement of the electric permittivity, submitted.

[33] X Xi, D.D.L. Chung, Electric permittivity of copper and its dependence on stress and surface oxidation, submitted.

[34] A.A. Eddib, D.D.L. Chung, Electric permittivity of carbon fiber, Carbon 43 (2019) 475–480.

[35] X Xi, D.D.L. Chung, Colossal electric permittivity discovered in polyacrylonitrile (PAN) based carbon fiber, with comparison of PAN-based and pitch-based carbon fibers, submitted.

[36] X Xi, D.D.L. Chung, Piezoelectric and piezoresistive behavior of unmodified carbon fiber, submitted.

[37] S. Wen, D.D.L. Chung, Cement-based materials for stress sensing by dielectric measurement, Cement Concr. Res. 32 (9) (2002) 1429–1433.

[38] A.A. Eddib, D.D.L. Chung, First report of capacitance-based self-sensing and in-plane electric permittivity of carbon fiber polymer-matrix composite, Carbon 140 (2018) 413–427.

[39] D.D.L. Chung, Processing-structure-property relationships of continuous carbon fiber polymer-matrix composites, Mater. Sci. Eng. R 113 (2017) 1–29.

[40] X. Hong, W. Yu, D.D.L. Chung, Electric permittivity of reduced graphite oxide, Carbon 111 (2017) 182–190.

[41] X. Hong, W. Yu, A. Wang, D.D.L. Chung, Graphite oxide paper as a polarizable electrical conductor in the through-thickness direction, Carbon 109 (2016) 874–882.

[42] X. Hong, W. Yu, D.D.L. Chung, Significant effect of sorbed water on the electrical and dielectric behavior of graphite oxide, Carbon 119 (2017) 403–418.

[43] X. Hong, D.D.L. Chung, Exfoliated graphite with relative dielectric constant reaching 360, obtained by exfoliation of acid-intercalated graphite flakes without subsequent removal of the residual acidity, Carbon 91 (2015) 1–10.

[44] A. Wang, D.D.L. Chung, Dielectric and electrical conduction behavior of carbon paste electrochemical electrodes, with decoupling of carbon, electrolyte and interface contributions, Carbon 72 (2014) 135–151.

[45] M. Moalleminejad, D.D.L. Chung, Dielectric constant and electrical conductivity of carbon black as an electrically conductive additive in a manganese-dioxide electrochemical electrode, and their dependence on electrolyte permeation, Carbon 91 (2015) 76–87.

[46] https://en.wikipedia.org/wiki/Electrical_resistivity_and_conductivity (as viewed on Sept. 29, 2018).

[47] X. Wang, D.D.L. Chung, Electromechanical behavior of carbon fiber, Carbon 35 (5) (1997) 706–709.

[48] https://www.amesweb.info/Materials/Poissons-Ratio-Metals.aspx (as viewed on Oct. 22, 2018).

[49] Teijin Carbon America, Inc., private communication.

[50] https://www.teijincarbon.com/fileadmin/PDF/Datenbl%C3%A4tter_en/Filament-Product_programm__EU__v27_2018-06-27_EN.pdf (as viewed on Sept. 29, 2018).

[51] http://ase.au.dk/fileadmin/www.ase.au.dk/Filer/Laboratorier_og_vaerksteder/Komposit-lab/Fiber/Carbon/Carbon_UD_HS__194_gsm__Tenax-E_HTS45_E23_-_TDS.pdf (as viewed on Sept. 22, 2018).

[52] http://pdf.directindustry.com/pdf/toho-tenax-europe-gmbh/tenax-e-hts45-p12-12k/37818-629937.html (as viewed on Sept.22, 2018).

[53] B. Pierozynski, On the hydrogen evolution reaction at nickel-coated carbon fibre in 30 wt. % KOH solution, Int J Electrochem Sci 6 (2011) 63–77.

[54] https://en.wikipedia.org/wiki/Nickel (as viewed on Dec. 28, 2018).

[55] https://xdevs.com/doc/Keithley/2002/SPEC-2002.pdf (as viewed on Sept. 22, 2018).

[56] N.S. Qu, D. Zhu, K.C. Chan, W.N. Lei, Pulse electrodeposition of nanocrystalline nickel using ultra narrow pulse width and high peak current density, Surf. Coating. Technol. 168 (2–3) (2003) 123–128.

[57] A.M. El-Sherik, J. Shirokoff, U. Erb, Stress measurements in nanocrystalline Ni electrodeposits, J. Alloy. Comp. 389 (1–2) (2005) 140–143.

[58] M. Sugimoto, R. Teranishi, S. Ooue, M. Mukaida, N. Mori, K. Yamada, H. Fukushima, T. Izumi, Y. Shiohara, Electrodeposition of textured nickel on nickel alloy Hastelloy, Physica C 469 (15–20) (2009) 1371–1373.

[59] L. Ma, K. Zhou, L. Zhang, Z. Li, A study on the oxidation behavior of nickel coatings with different grain sizes and preferred orientations, Adv. Mater. Res. 183–185 (2011) 1762–1766. Pt. 3, Environmental Biotechnology and Materials Engineering.

[60] https://en.wikipedia.org/wiki/Kramers%E2%80%93Kronig_relations (as viewed on Sept. 7, 2018).